CONTROL OF DOPANTS/MODIFIERS IN DIFFERENTIAL MOBILITY SPECTROMETRY USING A PIEZOELECTRIC INJECTOR

Victor Moll[1], Victor Bocoş-Binţinţan[1,2], Ileana-Andreea Raţiu[2], Dorota Ruszkiewicz[1] and C.L. Paul Thomas[1].

[1] Centre for Analytical Science, Department of Chemistry, Loughborough University, Loughborough, Leicestershire. LE11 3TU. UK

[2] "Babes-Bolyai" University, Faculty of Environmental Sciences, Str. Fantanele nr. 30, 400294 Cluj-Napoca, Romania.

Abstract

A piezoelectric injector has been interfaced to a differential mobility spectrometer to enable fast and reversible control of dopant/transport-gas modifier levels within the reaction region of the instrument. Operating at 1 Hz with optimised bipolar waveforms for the piezoelectric injector and gas flows within the injector, steady-state 2-butanol mass fluxes of 21 to 1230 ng min^{-1} and 1-bromohexane mass fluxes of 149 to 2644 ng min^{-1} were delivered to the differential mobility cell. Control of split-flow and transport-gas flow rates enabled rapid and flexible control of the dopant concentrations. The system was consistently reproducible with a relative standard deviation (RSD) of 7.9% at every mass- flux level studied. Stable responses were achieved between 3 to 5 seconds following a change in the control levels and no significant hysteresis effects were observed.

In the positive mode it was possible to control the extent of formation protonated monomer and proton bound cluster ions, tentatively assigned to $\{C_4H_9OH(H_2O)_n\}^+$ and $\{2C_4H_9OH(H_2O)_n\}^+$ and similar control was possible in the negative mode where the concentration relationship for the formation of bromide clusters indicated the presence of multiple ionisation mechanisms. A dopant formulation for the simultaneous control of ions in both the positive and negative modes was demonstrated by the injection of a 50%/50% v/v solution of 2-butanol/1-bromohexane with mass fluxes of 2-butanol in the mixture of between 11 and 1161 ng min^{-1} and between 13 and 1325 ng min^{-1} for 1-bromohexane.

Keywords: Differential mobility spectrometry, piezoelectric actuation, APCI control, dopant.

Introduction

Optimisation and control of the atmospheric pressure chemical ionisation (APCI) processes that occur in the reaction region of an ion mobility spectrometer are important elements in the development of ion mobility spectrometry (IMS) techniques and applications. The characterisation of analytes in complex matrices by IMS is often achieved through imparting selectivity to the APCI used to generate the product ions, and this is achieved by introducing gas-phase reagents, termed dopants, into the reaction region of the instrument. Dopants, and by inference transport-gas modifiers, are present at concentrations over the range 0.1 to 8000 mg dm^{-3} [1,2], and selectively react with hydrated protons from the ionisation source yielding alternative reagent ions, that generate alternative cluster ions with the analyte. The result is an enhanced analyte signal accompanied by reduced matrix interferences [3-6].

Dopants are usually selected to have a proton, or electron affinity, lower than that of the analyte and yet larger than potential interfering components in the sample. Preferential charge-transfer to analytes occurs forming clearly resolved and more intense product ions. An exemplar study of this approach described the enhanced detection of 19 organo-phosphorous compounds (OPCs) with addition of acetone and dimethyl sulphoxide (DMSO) over a reported concentration range 0.1 - 2 ppm(v)[sic]; suppressing 35 interference peaks [3].

Ammonia has also been used as a dopant for amines in aliphatic solvents and benzene [7] and more recently in chemical agent detectors [8]. Ammonia has also been used as a dopant to increase the analytical space for formaldehyde determination. Hydrated ammonium ions have shorter drift times than pure water based reactant ions. Formaldehyde product ions are difficult to resolve from water-based reactant ions, so by shifting the drift-time of the reactant ion peak to shorter times the analytical space is increased [9]. In contrast, nonylamine has been used as a dopant for biogenic amines with the reactant-ion peak having significantly longer drift times than the product ions generated by 1,4-butanediamine and 1,5-pentanediamine, once more increasing the analytical space available to the measurement [10]. Dopants have also been applied to enhance analytical responses in the negative ionisation mode, most notably with halogenated hydrocarbons in

explosives detection based on the formation of halogenated adduct ions resulting from dissociative electron capture of the halogen-containing hydrocarbon [11-13].

Neutral vapours may also be added to the drift gases, or transport gases, in the mobility system to impart selective changes to the mobility of the product ions, and in such applications the term “modifier” is used [14-16]. It is also possible to use the same vapour to act as a dopant and a modifier at the same time. Dichloromethane at 0.1 %(v)[sic] was used to enhance the resolution of chloride adduct ions produced by nine explosive compounds in differential mobility spectrometry [17]. A recent review provides a timely and highly-useful introduction and summary of the general area of dopants and modifiers [18].

Dopants and chemical modifiers are introduced into the gas-circuits of ion mobility instruments with permeation sources [4 and 19]. These devices generate stable gas-phase concentrations in the ion mobility systems for prolonged periods of operation. Nevertheless, permeation approaches are not flexible, only a single type of APCI chemistry may be generated in the system, and concentrations may not be changed in a dynamic manner. Rigorous optimisation for different analytes is impracticable, and an instrument once doped in this manner is restricted in what applications it may be used for.

The need for new experimental techniques to enable the study, and hence optimisation, of dopant systems was cogently stated by Jaroslaw Puton, Marjaana Nousiaine and Mika Sillanpaa in 2008 when they wrote [18]:

> *“The availability of information on doping for IMS is limited. Especially there is lack of data concerning quantitative aspects of doping. With small exceptions, the experimental data in hitherto published reports do not give answers to questions on the influence of dopant on detection sensitivity and optimal concentration of dopant. There is also lack of works concerning mathematical modelling of complicated sample ionisation processes and the estimation of dependence between concentrations of sample components and signal. The subsequent studies will provide theoretical analysis of selected problems of dopant usage as well as experimental material for verification of theoretical models.”*

This paper describes a study undertaken to demonstrate control of dopant/modifier/sample levels in the reaction region of a differential mobility spectrometer[a] (DMS). Of interest was the study of transitions between different ion-clusters as the concentration changed. For example between protonated monomer- and proton-bound dimer-ion dopant chemistries in the positive mode and halide ions and halide adduct ions in the negative mode. Finally, this work sought to establish the feasibility of simultaneously controlling the APCI in the positive and negative modes by using blended dopant formulations; something that has not previously been demonstrated.

Recently, an approach for optimising the injection of dopant liquids was described. A method for the rapid optimisation of piezoelectric (PZX)-injection of volatile liquids was demonstrated for five dopants (2-butanol, 1-chlorohexane, dichloromethane, acetone and 4-heptanone) [20] that were injected into an aspirating ion mobility spectrometer; concentrations in the range 20.5 - 270.2 μg m^{-3} [20 and 21]. (A comprehensive introduction to the theory and practice of piezoelectric injectors is covered in Ikeda's, "Fundamentals of Piezoelectricity" [22].) The RSD's of the dopants' various reactant ion peak intensities generated under the continuous operation of the PZX–injector ranged between 3% and 18%, depending on the dopant being injected. Further, transient dopant concentrations over the range 12.3 μg m^{-3} to 77 μg m^{-3} were generated under PZX-control with R^2 values in the range 0.991 - 0.998 for a least-squares regression between the reactant ion peak intensity and injected mass. Transient durations of approximately 6 s, compatible with the elution of a gas-chromatographic peak [20] were demonstrated.

Selection of dopants for this study.

The adoption of ion mobility approaches for gas-phase characterisation of chiral biomolecules is an area of growing interest [23], and 2-butanol was used in a landmark study demonstrating enantiomeric resolution of atenolol, serine, methionine, threonine, methyl r-lucopyranoside, glucose, penicillamine, valinol, phenylalanine, and tryptophan from their respective racemic mixtures [14]. The study of chiral 2-butanol interactions in the gas

[a] The theory and background to differential mobility spectrometry has been reviewed and described elsewhere [27 to 28].

phase will seek to establish the respective roles of ion-molecule reactions, and host-guest associations and control of the levels of this compound will be an important factor in such studies, hence its inclusion in this demonstration. An additional, and practical consideration, was the straightforward isolation of the ions formed by the addition of 2-butanol from the water-based reactant ions.

The practically of a resolved halide dopant ion at low concentration was the selection criterion for 1-bromohexane. Halogenated compounds are widely used in explosives detection, and usually these are chlorinates [17]. However chloride clusters are difficult to resolve from oxygen-based negative mode reactant ion signals, and as the dissociative ionisation of bromoalkanes in DMS have been observed to be similar/same as that of chloroalkanes a brominated compound was selected to allow the negative mode ions to be resolved and the operation of the system to be demonstrated in a straightforward way [24].

Experimental

Instrumental

A PZX-injector and interface was prepared from a PZX-injector (60 µm injection orifice diameter Microfab Technologies, Plano, TX, USA) controlled by a variable voltage waveform generator (AductorDrive™ III, Microfab Technologies). The control waveforms for the PZX-injector were created using proprietary software run on a Dell Studio 1737 lap top (Pentium Dual Core T4200 2 GHz processor, 2 Gb memory, 32-bit Windows Vista operating system). The PZX-injector [20] was fitted into a machined PTFE block (Albrook engineering, Loughborough, UK) through which purified air, (Varian Inc., Middleburg, Netherlands) was supplied and split into a clear glass GC injection liner (2 mm I.D. Supelco, Park Bellefonte, PA, USA), positioned 1 mm below the PZX-orifice tip. The internal chamber of the PTFE block and the gas-circuit within it promoted efficient transfer of droplets into a heated zone (100°C) where they evaporated and were efficiently mixed into the transport gas. Potential volatile interferences emanating from the PZX-injector were removed by a portion of the high-purity air supply acting as a curtain-flow, through which the droplets were injected. This gas-flow also purged the injection system; analogous to the septum purge in a gas chromatography injector.

If the back-pressures within this assembly were not maintained to the correct levels the injector did not operate correctly. To connect the injector outlet, at near-to-ambient pressure, to the pressurised transport gas inlet (108 kPa) of the DMS required a stainless-steel adductor-pump (Albrook Engineering, Loughborough, UK). The adductor-pump exploited the Venturi effect of the transport gas to ensure that the dopant-flow was maintained into the transport-gas from the evaporation zone [25 and 26].

<Figure 1 here>

Figure 1 is a schematic diagram of the layout and arrangement of the components used in the injector assembly. The DMS transport gas was purified and dried air ([H_2O] = 47.9 ± 0.3 μg m^{-3}; taken from a common supply that was also used for the PZX-injector. The inlet-flow to the adductor-pump (F5, Figure 1) was maintained at 600 cm^3 min^{-1} giving a capillary-flow (F4, Figure 1) of 5 cm^3 min^{-1}. The inlet flow to the DMS was regulated, if required, with a final split (F7, Figure 1) of 250 cm^3 min^{-1}, controlled with a needle valve, giving a transport gas-flow to the DMS cell (F8) of 355 cm^3 min^{-1}.

The DMS (Sionex Inc., Boston, MS, USA) was maintained at 80 °C with a 5.9 MBq ^{63}Ni ionisation source. The gap between the two parallel electrodes was 0.5 mm and detection was with off-axis positive and negative Faraday-plates. The dispersion-field ($\boldsymbol{E_D}$) strength was 21 kV cm^{-1}. The DMS spectra were captured at a rate of 1 Hz; the step size of the compensation-field ($\boldsymbol{E_c}$) scan was 11.8 V cm^{-1}, and each spectrum covered the range -0.8 kV cm^{-1} to 0.2 kV cm^{-1}. A virtual instrument (Sionex DMx Expert, version 2.4.0. run on the same lap-top specified above was used to control the DMS and record the data. The data were archived in .xls file format, they were processed and analysed with Microsoft Excel 2003.

Experimental Approaches

Two studies were run. The first characterised the DMS responses obtained from controlling the mass-fluxes of 2-butanol and 1-bromohexane generated from different solutions fitted to the PZX-interface. The second experiment characterised the responses observed from a 50:50 mixture of the dopants. The reagents used were obtained from Sigma, Gillingham, UK, and had purities >99.5%, and the general approach was the same for both studies.

1 cm³ of 2-butanol, or 1-bromohexane, or the dopant mixture, was placed into a 3 cm³ luer-lok syringe (CD Biosciences, Hamburg, Germany) that was fitted to the PZX-injector. A gas-line was attached to top of the syringe and a slight vacuum was applied (-2.6 kPa) to stabilise the liquid at the orifice tip and prevent the spontaneous expulsion of droplets. A statistically-optimised bipolar voltage waveform applied to the PZX-injector controlled the ejection of droplets into the heated evaporation zone [20]. The two compounds with their different physical properties (surface tension, viscosity) required different waveforms to produce precise droplet volumes. The protocol for efficiently creating such waveforms has been described recently [20] and a 4-factor, 2-centroid point, central composite design (CCD) was used as the experimental optimisation approach. The factors used in the optimisation were the dwell voltage ($\boldsymbol{V_d}$ / V), dwell time ($\boldsymbol{T_d}$ / µs), echo voltage ($\boldsymbol{V_e}$ / V) and echo time ($\boldsymbol{T_e}$ / µs) of the bipolar waveform, Table 1.

<Table 1 near here>

Individual droplets, with volumes in the range 50 - 120 pl were observed under stroboscopic lighting (Microfab Technologies, Plano, TX, USA) with a microscope (magnification: 200x), fitted with charge coupled device camera, positioned orthogonally to the ejection trajectory of the droplets. The optimisation was performed using multiple linear least squares to correlate the observed droplet characteristics of droplet volume V (estimated from the droplet radius) and droplet stability P to the factor levels of the (CCD) design, Equation 1.

$$\underline{P(\%) = \frac{\varphi(\mu m)}{\eta(\mu m)}} \qquad \textbf{Equation 1}$$

where $\boldsymbol{\varphi}$ was the droplet diameter and $\boldsymbol{\eta}$ was the displacement of the droplet orthogonal to the vertical ejection trajectory over the injection gap.

Once the waveforms had been optimised the PZX-injector was fitted into the PTFE-block and then the inlet gas-flow (F_1 in Figure 1) and the exhaust-flow (F_2 in Figure 1 were set to 200 cm³ min^{-1} and 30 cm³ min^{-1} respectively for all experiments. The waveform frequency to the PZX-injector was 1 Hz for both individual dopants and the dopant mixture. The dopant mass-

fluxes, Q (ng min^{-1}), entering the DMS cell were finessed by varying the split flows applied at two points before and after the adductor pump interface (F_3 and F_4 in Figure 1). Table 2 shows the dopant mass fluxes and concentrations (μg m^{-3}) entering the DMS cell at each level in the experiment.

<Table 2 near here>

Eight different mass-fluxes were studied for each dopant over the ranges 21 - 1230 ng min^{-1} for 2-butanol, and 149 - 2644 ng min^{-1} for 1-bromohexane. In the study using the dopant mixture, the mass ranges were 11 - 1161 ng min^{-1}, and 13 - 1325 ng min^{-1} for 2-butanol and 1-bromohexane, respectively. Each mass-flux level (Q) was maintained for 20 s while DMS spectra were recorded. The test started at zero flux before the mass-flux was sequentially increased to the maximum level at which point the sequence was reversed and the mass-flux was reduced sequentially back to zero.

Table 3 summarises the DMS settings that were used. The dispersion-field level was chosen to generate the maximum product ion peak- intensity consistent with peak resolution for all the ions of interest. The data from the DMS were background subtracted and baseline shifted before the ion peaks were integrated.

<Table 3 near here>

Results and Discussion

Experiments 1 and 2. Single dopant test sequences and their responses

Figure 2 shows a response surface obtained as the mass flux of the 2-butanol was successively increased and then decreased. Beneath the response surface are three differential mobility spectra obtained at different dopant fluxes, indicated by dotted lines. Without the addition of 2-butanol a water-based reactant ion peak was observed at ca. -400 V cm^{-1} and at mass-fluxes of 2-butanol between 21 and 514 ng min^{-1}, a product ion signal was observed at a compensation field ($\boldsymbol{E_c}$) of -166.6 V cm^{-1}. At mass-fluxes above 514 ng min^{-1} a larger product ion was observed at an $\boldsymbol{E_c}$ value of -75 V cm^{-1}, and the intensity of the peak at $\boldsymbol{E_c}$ = -166.6 V cm^{-1} reduced until Q > 704 ng min^{-1} where it was no longer observed. From this level until the maximum level of Q = 1230 ng min^{-1} the second peak at $\boldsymbol{E_c}$ = -75 V

cm^{-1} continued to increase in intensity, with a corresponding reduction in the reactant ion peak ($\boldsymbol{E_c}$ = -400 V cm^{-1}). This behaviour is characteristic of monomer/dimer product ion formation of alcohols in APCI systems [29] in the positive ionisation mode following the scheme in (Reaction 1).

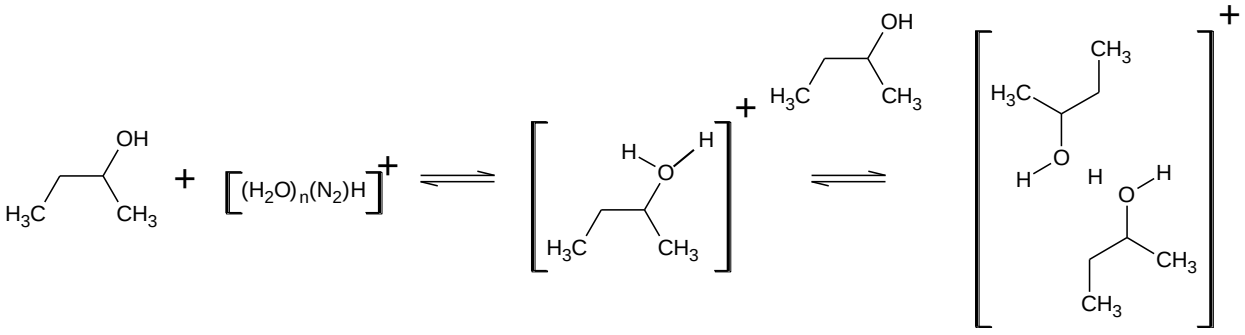

Reaction 1. Protonated monomer and proton bound dimer formation with increasing mass-flux of 2-butanol. Note water and permanent gas components of the cluster ions left out for clarity.

<Figure 2 near here>

The feature observed at a compensation field of -166.6 V cm^{-1} (Bottom DMS spectra taken from the Left-Hand Section of the response surface in Figure 2) may be tentatively assigned to the formation of a protonated monomer ion. Increasing the concentration in the reaction region was accompanied by the appearance of an additional peak at -75 V cm^{-1} (Middle DMS spectra taken from the Right-Hand Section of the response surface in Figure 2) thought to be due to the formation of a proton-bound dimer cluster ion. As the concentration of 2-butanol was increased, the peak at -75 V cm^{-1} became dominant (Top DMS spectra taken from the Middle Section of the response surface in Figure 2) indicative of the quantitative production of proton-bound dimer ions. The relationship between 2-butanol mass-flux/concentration and ion-yields observed in these experiments is summarised in Figure 3. Figure 3 also indicates the extent of the control of the monomer and dimer abundance that may be achieved, and interestingly, also indicates a loss of charge from the system; integrated ion intensity reduces with increasing mass-flux of 2-butanol. Dehydration of protonated 2-butanol in the gas phase has been reported to occur, largely yielding a

racemic mixture of 2- butene. Proton bound dimers have been found to eliminate water to yield the corresponding protonated dialkylether [30].

<Figure 3 near here>

Figure 4 shows the negative mode ion data in a similar layout to Figure 2. In the absence of 1-bromohexane just an oxygen-based reactant ion peak was present at a compensation field of ca. -400 V cm^{-1}, (Bottom DMS spectra taken from the Left-Hand Section of the response surface in Figure 4). Introduction of 1-bromohexane generated a feature at a compensation field of -356.2 V cm^{-1}, that was partially resolved from the oxygen-based reactant ion (Middle DMS spectra taken from the middle section (at a scan time of 30 s) of the response surface in Figure 4) As the mass/flux of 1-bromohexane was increased the original reactant ion was depleted completed while the bromide cluster increased in intensity (Top DMS spectra taken from the Right-Hand Section (at a scan time of 75 s) of the response surface in Figure 4).

The mass-flux/signal relationship in the negative mode with 1-bromohexane doping, Figure 5, shows an apparent discontinuity at a mass-flux of 149 ng min^{-1}, perhaps indicative of the presence of two ionisation mechanisms. The compensation field of the ion cluster observed at a compensation field of -356.2 V cm^{-1} is thought to be due to a bromide cluster formed through dissociative ionisation [24]. At mass fluxes below 149 ng min^{-1} ("A" in Figure 5) the loss of oxygen-based reactant ions was inversely proportional to the yield of bromide ions, and this is indicative of charge transfer from the oxygen reactant ions to 1-bromohexane followed by dissociation. As the mass flux increased the rate of production of bromide clusters reduced and tended towards a linear function until at a flux at 1.92 µg min^{-1} the yield of bromide clusters exceeded the initial level of the undoped oxygen-based reactant ions. Two comments arise from these observations. Firstly, there appear to be at least two distinct ionisation mechanisms involved in the production of bromide. Secondly, this demonstration-test indicated nuanced complexity in concentration dependent halide dopant chemistries; a subject for future studies.

<Figures 4 and 5 near here>

Figure 6 illustrates the stability and dynamics observed for the demonstration test sequences used for Experiments 1 and 2. The precision of the observed responses for both

dopants across at all settings fell between 1.2% and 7.9% RSD,. The switching speed between concentrations, described in terms of stabilisation time, was between 3 and 5 s. The transit time though the injector was approximately 800 ms and the lag is thought to be attributable to adsorption phenomenon onto the internal surfaces of the gas-lines and adductor pump

<Figure 6 near here>

Experiment 3 Dopant formulation with simultaneous positive and negative mode doping.

The 50:50 solution of 2-butanol and 1-bromohexane was loaded and injected to study the responses observed with simultaneous dopant injection for the positive and negative modes, see Figure 7. In the positive mode, the protonated 2-butanol monomer and dimer ion clusters were observed at compensation fields of -166.6 V cm^{-1} and -75 V cm^{-1}, respectively; identical compensation fields to those observed from single dopant injections. The same findings were obtained in the negative mode with the bromide cluster observed at a compensation field of -397.6 V cm^{-1}. No other product ions were observed in either ionisation mode. Plots of mean ion signal intensity vs Q in Figure 8 enable comparison of the responses observed with the dopant mixture against that seen with the single dopants.

<Figure 7 and 8 near here>.

The relationship between the intensity of the ion signal and the mass-flux of dopant was estimated by linear regression for the single dopant studies (Experiments 1 and 2) and the mixed dopant study (Experiment 3), and the parameters for 2-butanol and 1-bromohexane ions are summarised in Tables 4 and 5 respectively. The responses observed in the single dopant and mixed dopant tests were essentially equivalent within the limits of the precision of the injection-system. There was no evidence of the mixed dopants interfering with the generation of ions in the opposite polarity mode. The positive and negative ionisation processes could be doped independently of one another using a formulated mixture.

Conclusions

These studies suggest that using a PZX-approach to control dopant chemistry within APCI-based detection systems is feasible. Further, the potential of combining dopants for

different modes of operation has also been explored. The full utility of controlling the precise nature of the dopant ions in in mobility and mass spectrometric inlets has yet to be investigated; nonetheless such studies are now practicable. Straightforward control of injection, and gas-flows enabled dopant levels and chemistries to be set and controlled within seconds, and the approach was amenable to automated parametric control. In the course of this study the rapid concentration programming of test compounds revealed complexity that justify hyphenation to a mass spectrometer to enable ions assignments to be made with a greater level of certainty. This will be the subject of future studies.

This technique appears suitable for use in controlling the level of water (as part of a formulated dopant mixture perhaps) and the concentration of drift-gas/transport gas modifiers in future studies. The miniaturisation and optimisation of the design for closer integration into the gas circuits of a range of mobility platforms, including hyphenated chromatography-mobility combinations are a logical continuation of this study. “Drop-on-demand” dopant systems will enable the optimisation and refinement of multiple analyte responses over the course of chromatographic runs. PZX-actuation approaches appear to be a reliable and workable approach to the efficient exploration of APCI control in instrumental systems that go beyond ion mobility.

Acknowledgements

Ileana-Andreea Ratiu wishes to thank for the financial support provided from programs co-financed by The SECTORAL OPERATIONAL PROGRAMME HUMAN RESOURCES DEVELOPMENT, Contract POSDRU 6/1.5/S/3 – „Doctoral studies: through science towards society".

All the authors wish to thank John Hogg Technical Solutions, Trafford Park, Manchester; Shell Global Solutions, Thornton Research Park, Cheshire; and the Technology Strategy Board, UK, for their financial support of the project. Special thanks are also offered to Richard Harrison from Ernst and Young who acted as our project manager.

References

[1] Q. Meng, Z. Karpas, and G. A. Eiceman, *Int. J. Env. Anal. Chem*., 1995, **61,** 81.

[2] D. S. Levin, R. A. Miller, E. G. Nazarov, and P. Vouros, *Anal. Chem.,* 2006, **78,** 5443.

[3] G. A. Eiceman, Y-F. Wang, L. Garcia-Gonzalez, C. S. Harden, and D. B. Shoff, *Anal. Chim. Acta*., 1995, **306**, 21.

[4] M. Jafari, *Talanta*, 2006, **69,** 1054.

[5] T. Khayamian, M. Tabrizchi, and M. Jafari, *Talanta*, 2006, **69,**795.

[6] G. A. Eiceman and Z. Karpas, "Ion Mobility Spectrometry" Second Edition, Publ. CRC Press, Boca Raton, Fl., USA, 2005.

[7] S. Kim, F. W. Karasek, and S. Rokushika, *Anal. Chem*., 1978, **50**, 152.

[8] C. A. Hill and C. L. P. Thomas, *Analyst*, 2002, **128**, 55.

[9] J. Leonhardt, *J. Radioanal. Nucl. Chem*., 2003, **257**, 133.

[10] Z. Karpas, W. Chaim, R. Gdalevsky, B. Tilman and A. Lorber, *Anal. Chim. Acta*, 2002, **474**, 115.

[11] F. Karasek, O. Tatone, and D. Denney, *J. Chrom*., 1973, **87**. 137.

[12] C. Proctor, and J. Todd, *Anal. Chem*., 1984, **56**, 1794.

[13] K. Daum, D. Atkinson, R. Ewing, W. Knighton, and E. Grimsrud, *Talanta*, 2001, **54**, 299.

[14] P. Dwivedi, C. Wu, L. M. Matz, B.H. Clowers, W.F. Siems, and H. H. Hill. *Anal. Chem.* 2006, **78**, 8200.

[15] L. M. Matz, H. H. Hill, L. W. Beegle, I Kanik, *J. Am. Soc. Mass Spectrom*. 2002, **13**, 300.

[16] P. Dwivedi, C. Wu, L. M. Matz, B. H. Clowers, W. F. Siems, and H. H. Hill, *Anal. Chem*., 2006, **78**, 8200.

[17] G. A. Eiceman, E. V. Krylov, and N. S. Krylova, *Anal. Chem*., 2004, **76**, 4937.

[18] J. Puton, M. Nousiainen, and M. Sillanpaa, *Talanta*, 2008, **76**, 978.

[19] Y. Long, Y. Guo, and M. Lu, Rev. *Anal. Chem*., 2000, **19**, 179.

[20] V. H. Moll, V. Bocoş-Binţinţan, J. Chappell, D. Hutt, I-A. Ratiu and C. L. P. Thomas, *Int. J. Ion Mob. Spec.,* 2010, **13**, 149.

[21] V. H. Moll, V. Bocoş-Binţinţan and C.L.P. Thomas. UK Patent Application No: 1008286.5. 2010.

[22] T. Ikeda, "Fundamentals of Piezoelectricity", Publ. Oxford University Press, Oxford, UK, 1990.

[23] J. R. Enders and J. A. Mclean, *Chirality*, 2009, **21**, E253.

[24] G. R. Lambertus, C. S. Fix, S. M. Reidy, R. A. Miller, D. Wheeler, E. Nazarov, and R. Sacks, *Anal. Chem*., 2005, **77**, 7563.

[25] F. Durst, “Fluid Mechanics: An Introduction to the Theory of Fluid Flows”, Publ. Springer-Verlag, Berlin, Germany, 2008.

[26] M. Lehner, *Aerosol Sci. Tech*., 1998, **28**, 389.

[27] R. Guevremont, *J. Chrom. A*., 2004, 1058, 1.

[28] A. A. Shvartsburg, “Differential Ion Mobility Spectrometry”, CRC Press, Boca Raton, FL, USA. 2009

[29] R. G. Ewing, G. A. Eiceman, J..A. Stone, *Int. J. Mass Spect*. 1999, **193,** 57.

[30] J. L. Beauchamp and M. C. Caserio, J. Am. Chem. Soc., 1972, **94**, 2638.

AN-ART-11-2011-016109 TABLES AND FIGURES.DOCX

CONTROL OF DOPANT CHEMISTRY IN DIFFERENTIAL MOBILITY SPECTROMETRY USING A PIEZOELECTRIC ACTUATOR

FIGURES AND TABLES

Victor Moll[1], Victor Bocoş-Binţinţan[1,2], Ileana-Andreea Raţiu[2], Dorota Ruszkiewicz[1] and C.L. Paul Thomas[1]

1 Centre for Analytical Science, Department of Chemistry, Loughborough University, Loughborough, Leicestershire. LE11 3TU. UK

2 "Babes-Bolyai" University, Faculty of Environmental Sciences, Str. Fantanele nr. 30, 400294 Cluj-Napoca, Romania

Table 1 A summary of the central composite design factorial levels used to optimise the piezoelectric actuation parameters for 2-butanol (A) and 1-bromohexane (B).

	V_d / V		t_d / µs		V_e / V		t_e / µs		R²	v / pl	m / ng	P(%)
	L	Opt.	L	Opt.	L	Opt.	L	Opt.				
A	32.0 17.0	30.0	18.0 10.0	14.0	-0.5 -2.5	-1.0	3.0 1.0	1.5	0.90	61±4	49±3	6.6
B	24.0 16.0	19.1	24.0 14.0	20.2	-1.0 -3.0	-1.5	3.0 1.0	3.0	0.88	51±2	60±2	3.6
A + B	16.0 30.0	24.0	20.0 10.0	18.4	-0.5 -3.0	-1.5	3.0 1.0	3.0	0.92	54±3	25.22 (A) 28.78 (B)	5.5

Key: L: maximum and minimum limits of optimisation study; opt.: predicted optimised level; abs. R^2 correlation of model predictions to experimental variables. . V_d: dwell voltage; t_d: dwell time: V_e: Echo voltage; t_e: echo time; v: droplet volume; m: mass of droplet; P: droplet stability, (Equation 1).

Table 2 PZX interface parameters required for obtaining the mass fluxes and DMS dopant concentrations in this study. Exp. Is the experiment number, where 1 represents separate injections of 2-butanol (A), 2 represents separate injections of 1-bromohexane (B) and 3, the dopant mixture. $[D]$ is the dopant concentration entering the DMS cell.

Exp.	Q / ng min^{-1}		$[D]$ / µg m^{-3}		F_3 split ratio	F_4 flow / cm^3 min^{-1}
	A	B	A	B		
1	0		0		N/A	N/A
	21		17		151.5	0.8
	132		106		24.9	5.9
	244		195		9.3	10.9
	514		411		5.1	22.9
	704		563		3.9	31.3
	969		775		2.8	43.1
	1230		984		2.3	54.7
2		0		0	N/A	N/A
		149		119	21.4	5.2
		512		410	7.5	17.8
		904		723	4.1	31.4
		1229		983	2.8	42.7
		1602		1282	2.2	55.6
		1918		1534	1.9	66.6
		2644		2115	1.2	91.8
3	0	0	0	0	N/A	N/A
	11	13	9	10	130.0	1.0
	83	95	66	76	20.2	6.2
	292	333	234	266	6.0	20.8
	562	641	450	513	2.5	50.0
	750	856	600	685	2.3	54.3
	865	987	692	790	1.8	69.4
	1161	1325	929	1060	1.3	96.2

Table 3 DMS instrumental parameters used in this study

Parameter	Level
Transport gas	Filtered compressed air
Transport gas flow rate	355 cm^3 min^{-1}
DMS cell temperature	80 °C
Absolute humidity	47.9 ± 0.3 ppm
Dispersion field	21 kV cm^{-1} (for all dopants)
Compensation field scan range	-860 V cm^{-1} to 300 V cm^{-1}
Scan frequency	1 Hz
Scan step	11.8 V cm^{-1}

Table 4 Summary of linear regression parameters for control of ion signal intensities in the positive and negative modes.

Expt	Proposed Ion cluster	B_0 / mV	B_1 / mV min ng^{-1}	R^2	n
1	$\{(H_2O)_n(C_4H_{10}O)_2H\}^+$	-3.73	0.16	0.99	8
	$\{(H_2O)_nH\}^+$	343.3	-0.28	0.99	8
3	$\{(H_2O)_n(C_4H_{10}O)_2H\}^+$	0.13	0.17	0.99	8
	$\{(H_2O)_nH\}^+$	337.1	-0.3	0.98	8
2	$\{(H_2O)_nBr\}^-$	-20.57	0.063	0.97	8
	$\{(H_2O)_nO_2\}^-$	113	-0.049	0.91	8
3	$\{(H_2O)_nBr\}^-$	18.44	0.07	0.96	8
	$\{(H_2O)_nO_2\}^-$	119.5	-0.07	0.95	8

$$I(\text{mV}) = B_0(\text{mV}) + B_1\left(\text{mV min ng}^{-1}\right) \times Q\left(\text{ng min}^{-1}\right)$$

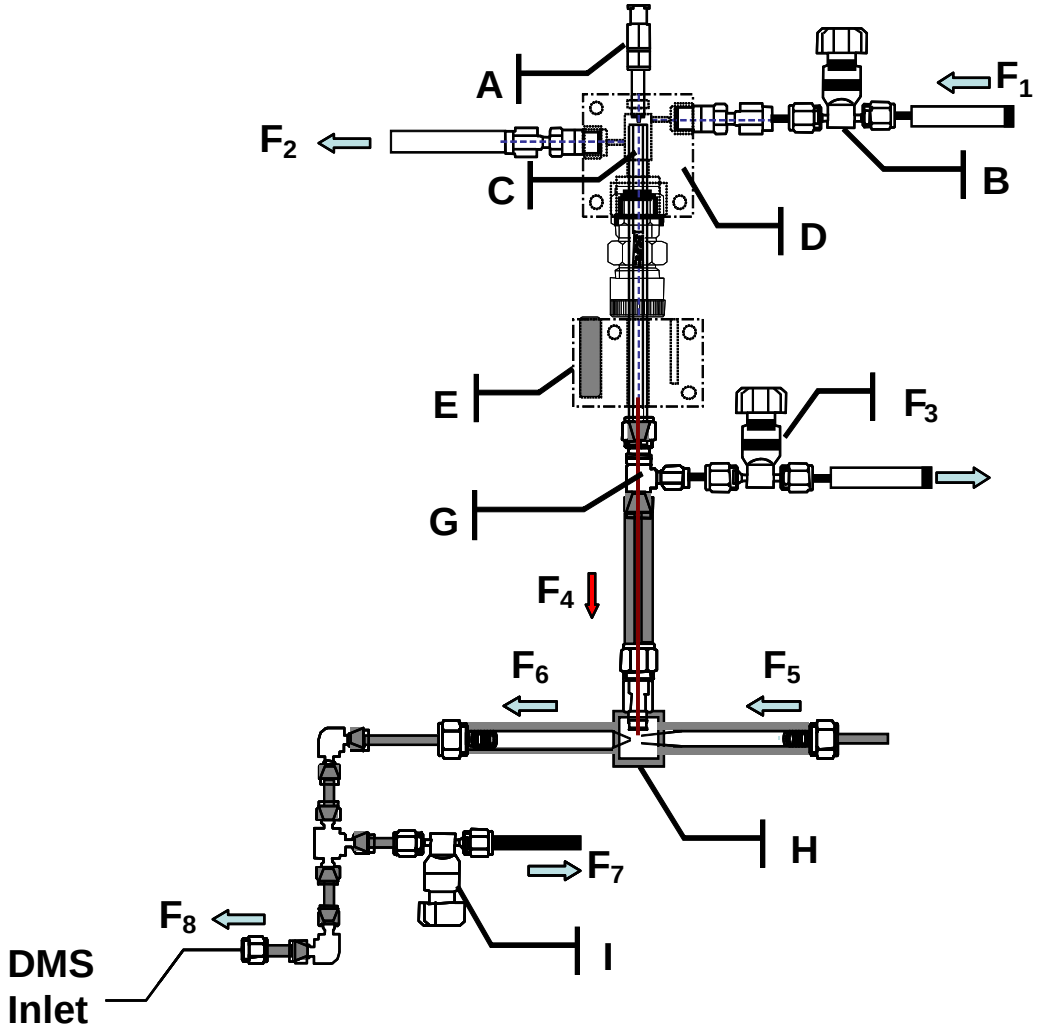

Figure 1. The actuator interface used in this study. A piezoelectric actuator ejected droplets, of controlled mass, of liquid dopant into a carrier gas stream of purified air. The aerosol was evaporated inside a heated glass liner housed within a PTFE block. The resultant mixture was split into a transfer line of deactivated silica capillary tubing connected to a Venturi jet-pump. Additional flow-control was achieved from a final split to before the DMS inlet.

Key: A: Piezoelectric actuator; B: needle valve; C: Injection liner; D: PTFE housing; E: Aluminium heating block; F: split flow controlled by needle valve; G: ultra-torr compression union; H: jet pump; and, I: split-flow controlled by needle valve. F_1, F_2, F_3 and F_4 are the flows relating to the inlet, the exhaust, the split and the capillary through the interface, respectively. F_5, F_6, F_7 and F_8 represent the jet-pump inlet flow, the outlet flow, the secondary split flow and the total DMS cell flow.

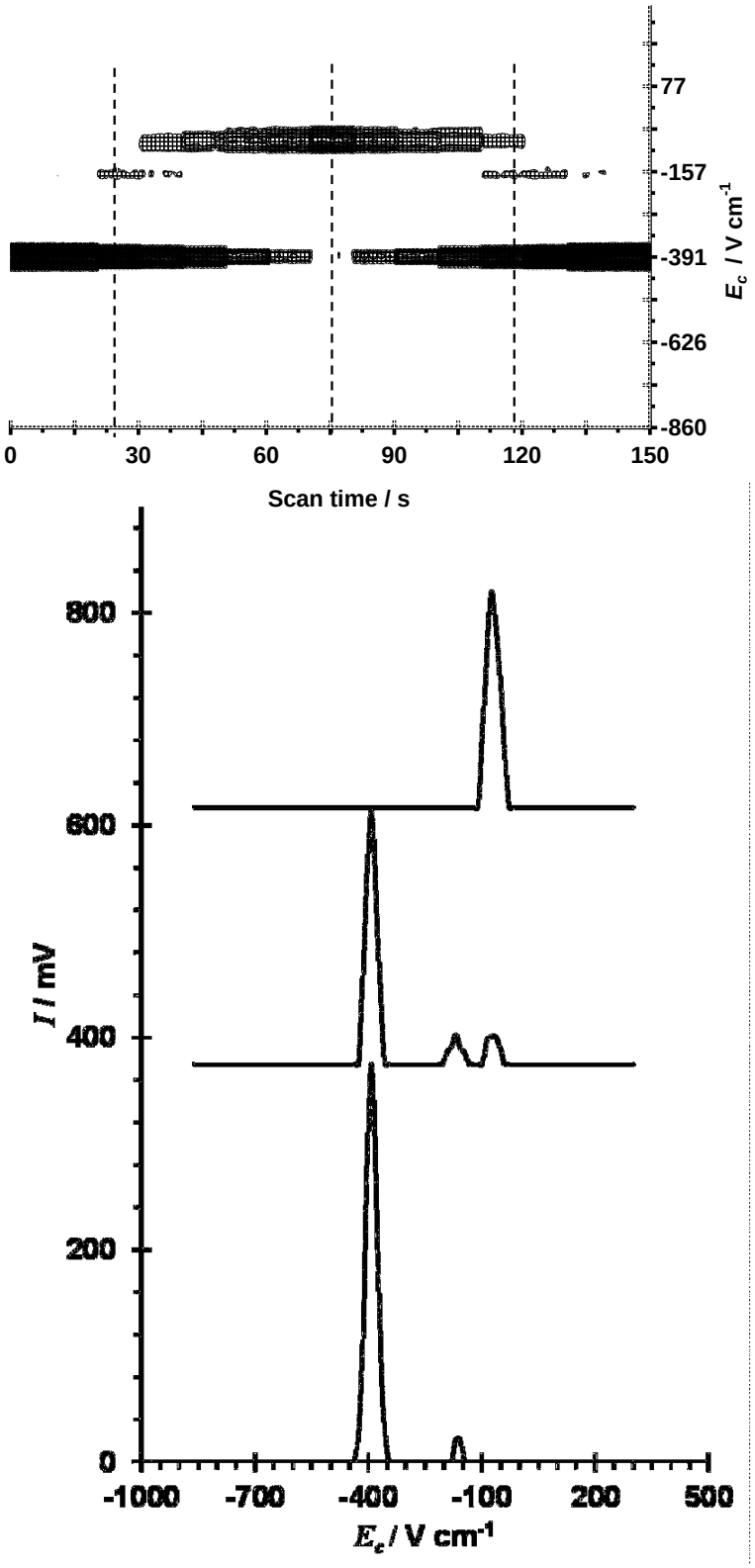

Figure 2 Top is the response surface from Experiment 1, with background-corrected, filtered and offset DMS spectra, bottom. Key: left and bottom: Water RIP and protonated monomer 2-butanol ion; middle and top: proton bound dimer 2-butanol ions, and right and middle: Water RIP, with protonated monomer 2-butanol ion and proton bound dimer 2-butanol ions.

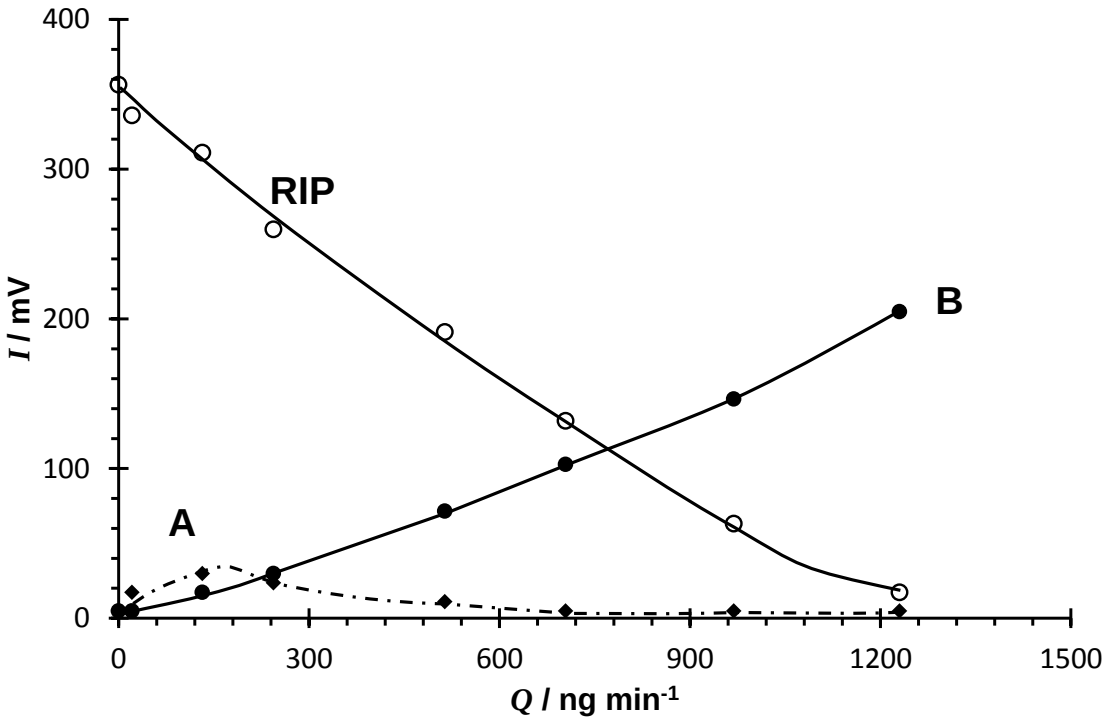

Figure 3 Plots of mean ion signal intensity vs 2-butanol mass flux. A depicts the responses arising from the ion cluster observed at a compensation field of -168 V cm^{-1}; assigned to a protonated monomer ion cluster. B is the trace associated with the larger ion cluster observed at -85 V cm^{-1}, though to be a proton bound dimer ion.

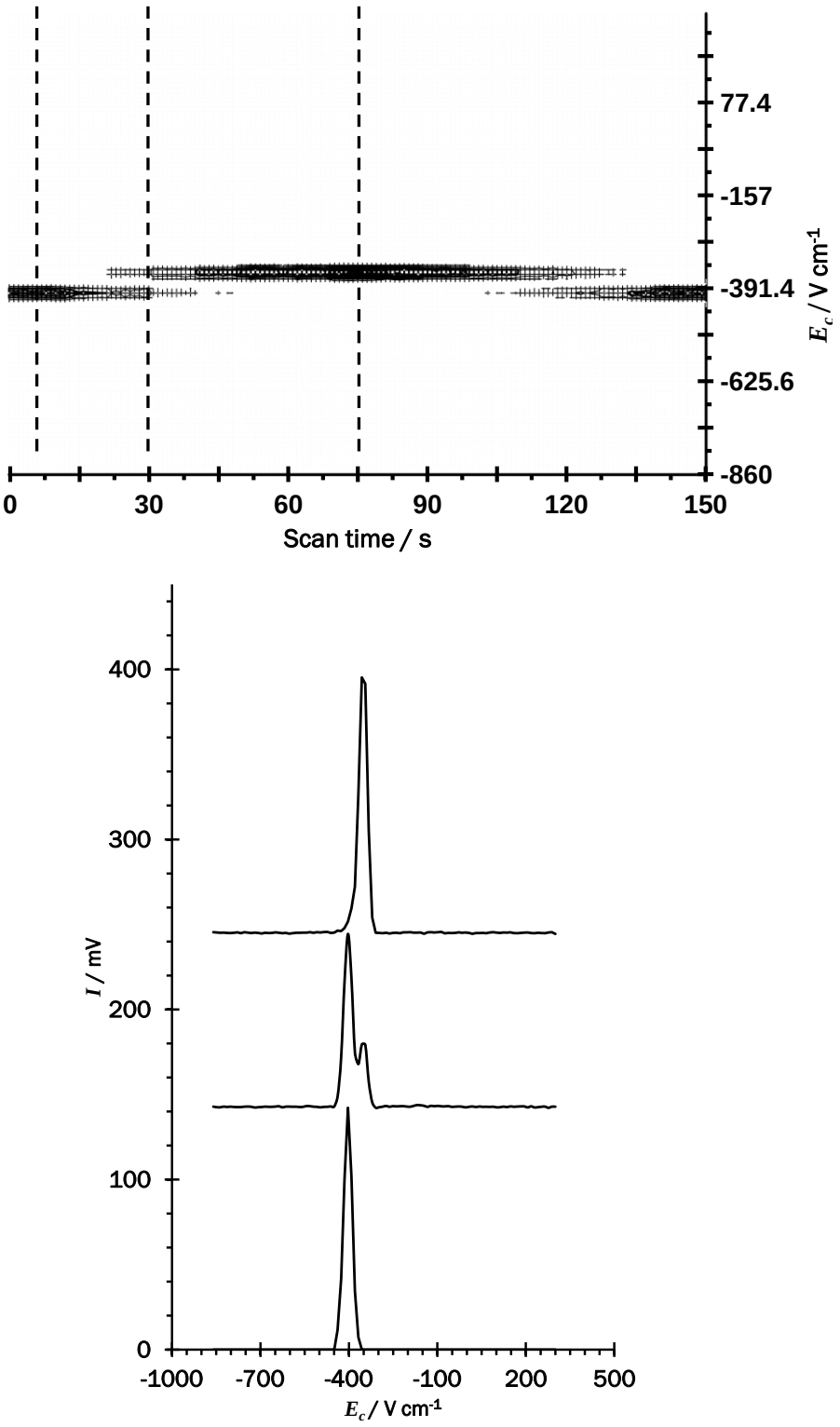

Figure 4 Top is the response surface from Experiment 2, with background-corrected, filtered and offset DMS spectra, bottom. Key: left and bottom: oxygen RIP; middle: mixed oxygen RIP and bromide ion; and, right and top: bromide ion.

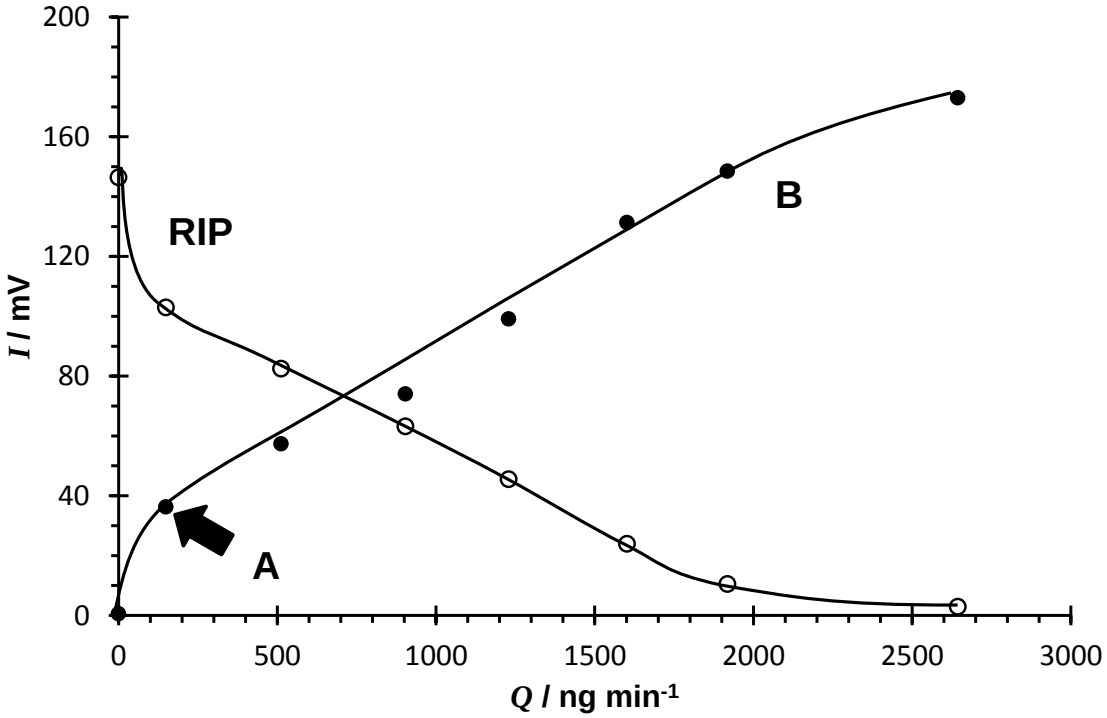

Figure 5 Response vs dopant concentration relationships from actuations of 1-bromohexane. A represents the region of proposed collision-based charge transfer, and B, direct ionisation of the dopant for at this mass-flux the intensity of the signal exceeded the intensity of oxygen RIP observed in an undopd system.

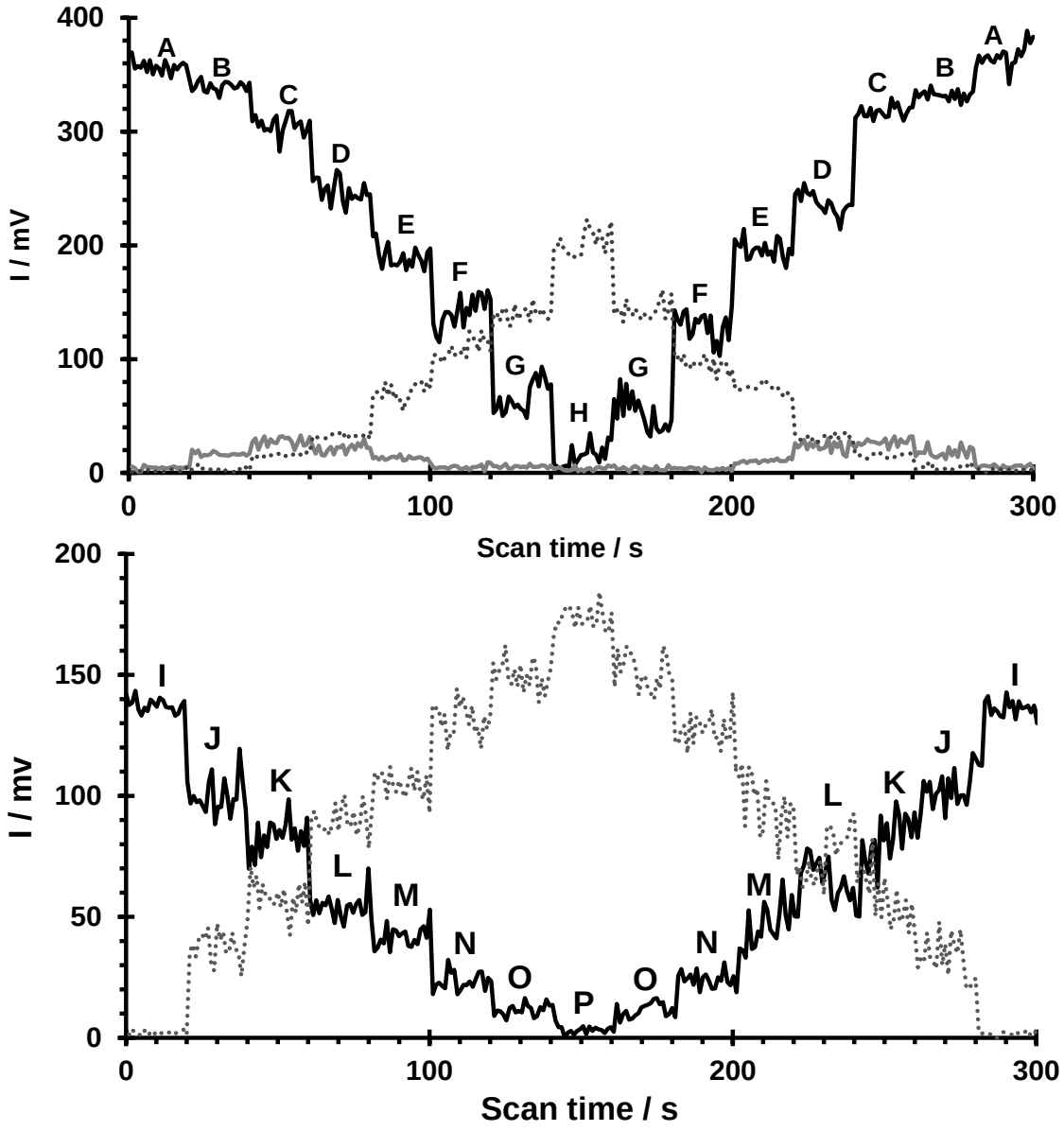

Figure 6 Plots of reactant and product ion signal intensity vs scan time for changing dopant fluxes into the DMS cell. Top: 2-butanol and bottom: 1-bromohexane. Key : 2-butanol, mass-fluxes in ng min^{-1}: A = 0, B = 21, C = 132, D = 244, E = 514, F = 704, G = 969, H = 1230. The RIP intensity is represented by the continuous black line, the proposed alcohol monomer by the continuous grey line, and the proposed proton-bound dimer ion by the dotted grey line. For 1-bromohexane injections : I = 0, J = 149, K = 512, L = 904, M = 1229, N = 1602, O = 1918, P = 2644. The oxygen RIP intensity in the negative mode is represented by the black continuous line, and the proposed bromide product, by the dotted grey line.

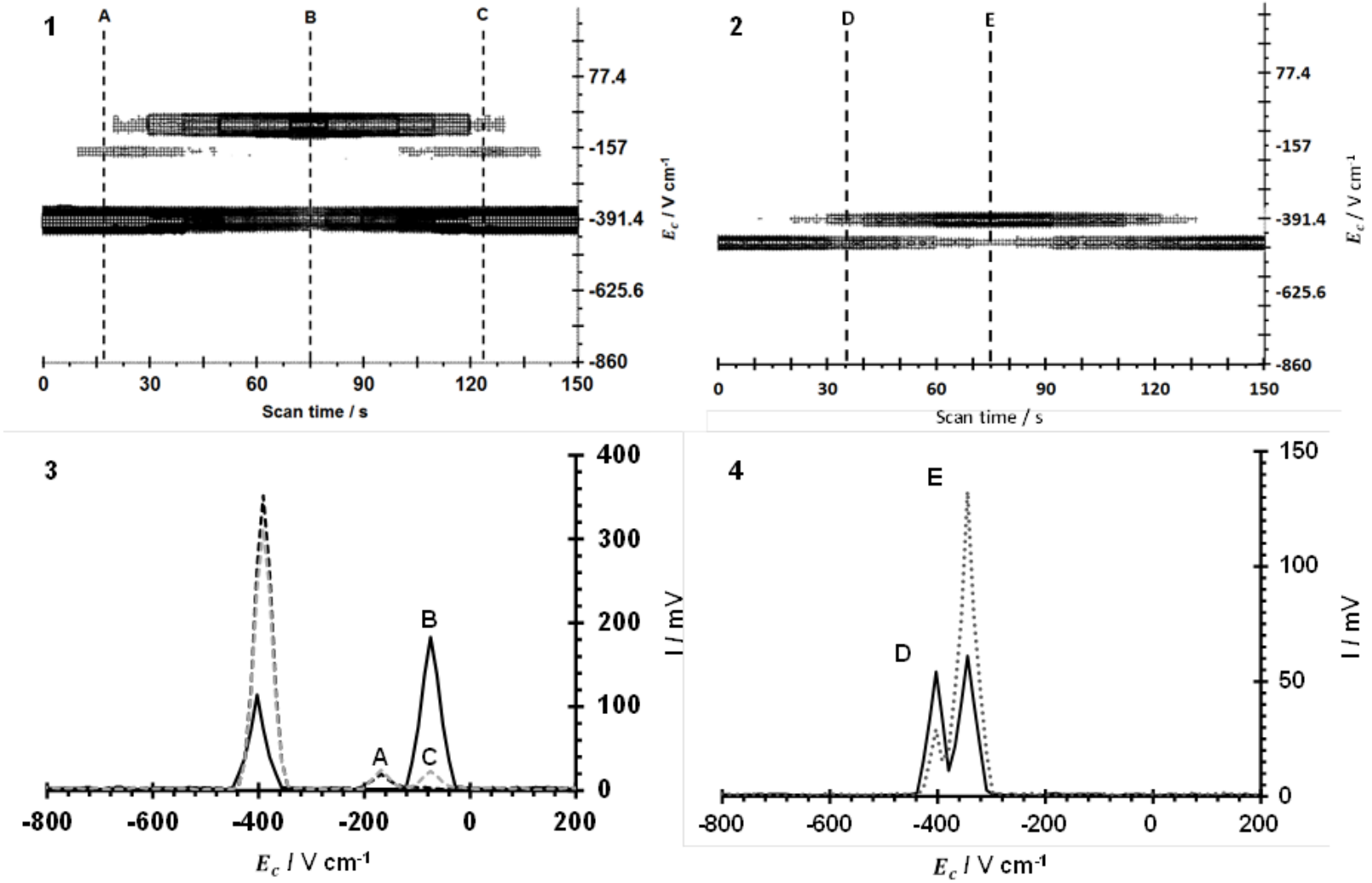

Figure 7 Responses for Experiment 3, 50: 50 2-butanol:1-bromohexane mixture. Graphs 1 and 2: positive and negative mode responses respectively. Graphs 3 and 4: selected DMS spectra from the positive and negative modes respectively. Key. A: protonated 2-butanol and hydrated proton RIP; B: proton bound 2-butanol dimer ion; and C: a mixture of all three positive mode ions; D: negative mode O_2^- based RIP and bromide ion; and E, direct dissociative electron capture of 1-bromohexane.

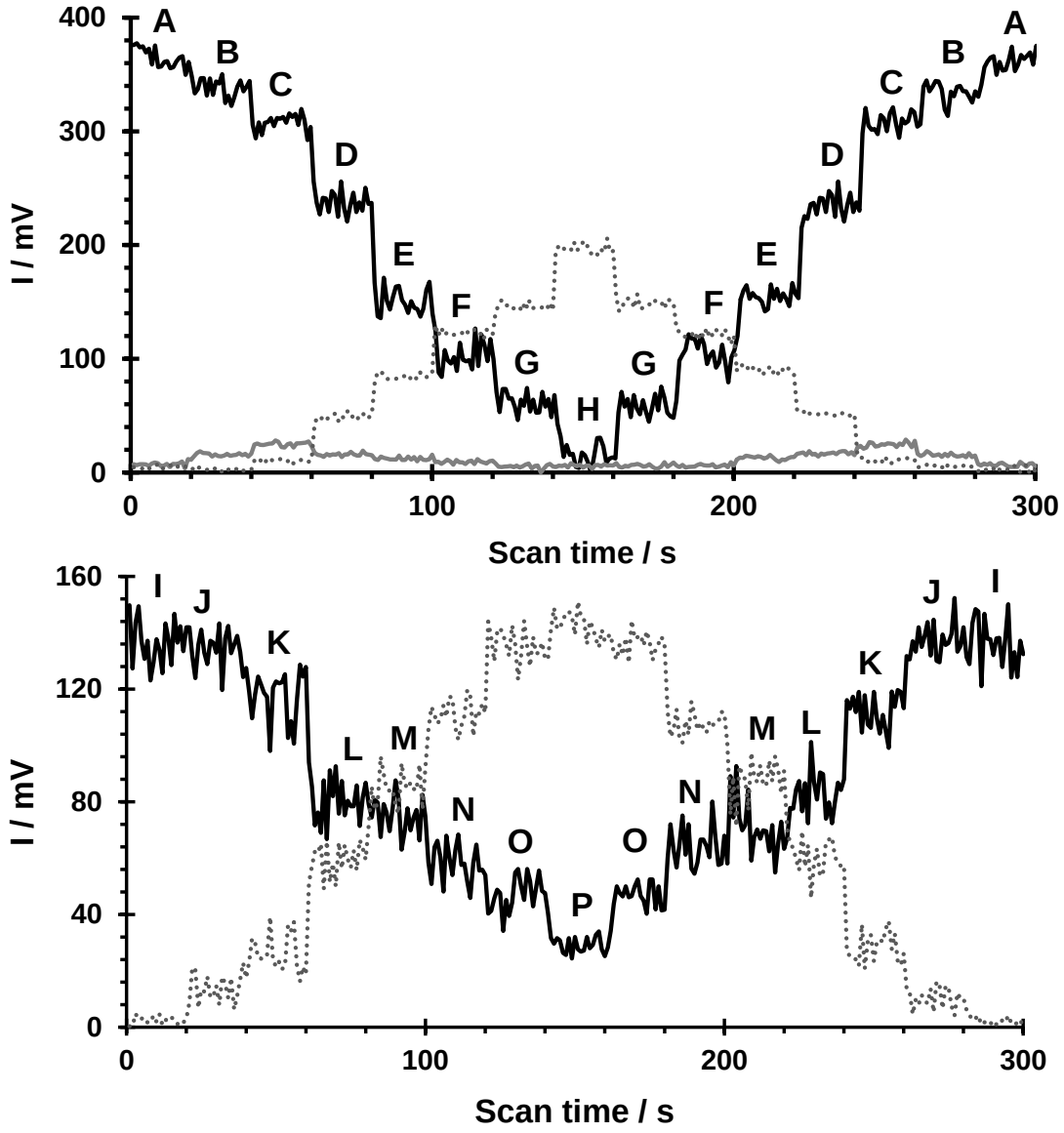

Figure 8 Plots of reactant and product ion signal intensity vs scan time for changing dopant mass fluxes at the DMS cell from actuation of the dopant mixture. The top graph relates to responses in the positive mode, and the bottom graph, in the negative mode. In the positive mode, the letters represent the following mass fluxes of 2-butanol, in ng min^{-1}: A = 0, B = 11, C = 83, D = 292, E = 562, F = 750, G = 865, H = 1161. In the negative mode, the letters represent the following mass fluxes of 1-bromohexane: I = 0, J = 13, K = 95, L = 333, M = 641, N = 856, O = 987, P = 1325.